EINDHOVEN UNIVERSITY OF TECHNOLOGY

LPE of InP and InGaAsP on InP substrates : a verification of the diffusion limited growth model

Citation for published version (APA):
Thijs, P. J. A., Nijman, W., & Metselaar, R. (1986). LPE of InP and InGaAsP on InP substrates : a verification of the diffusion limited growth model. *Journal of Crystal Growth*, *74*(3), 625-634. https://doi.org/10.1016/0022-0248(86)90209-5

DOI:
10.1016/0022-0248(86)90209-5

Document status and date:
Published: 01/01/1986

Document Version:
Publisher's PDF, also known as Version of Record (includes final page, issue and volume numbers)

Please check the document version of this publication:

• A submitted manuscript is the version of the article upon submission and before peer-review. There can be important differences between the submitted version and the official published version of record. People interested in the research are advised to contact the author for the final version of the publication, or visit the DOI to the publisher's website.
• The final author version and the galley proof are versions of the publication after peer review.
• The final published version features the final layout of the paper including the volume, issue and page numbers.

Link to publication

General rights
Copyright and moral rights for the publications made accessible in the public portal are retained by the authors and/or other copyright owners and it is a condition of accessing publications that users recognise and abide by the legal requirements associated with these rights.

• Users may download and print one copy of any publication from the public portal for the purpose of private study or research.
• You may not further distribute the material or use it for any profit-making activity or commercial gain
• You may freely distribute the URL identifying the publication in the public portal.

If the publication is distributed under the terms of Article 25fa of the Dutch Copyright Act, indicated by the "Taverne" license above, please follow below link for the End User Agreement:

www.tue.nl/taverne

Take down policy
If you believe that this document breaches copyright please contact us at:

openaccess@tue.nl

providing details and we will investigate your claim.

Download date: 15. Jul. 2024

Journal of Crystal Growth 74 (1986) 625–634
North-Holland, Amsterdam

LPE OF InP AND InGaAsP ON InP SUBSTRATES; A VERIFICATION OF THE DIFFUSION LIMITED GROWTH MODEL

P.J.A. THIJS, W. NIJMAN and R. METSELAAR *

Philips Research Laboratories, 5600 JA Eindhoven, The Netherlands

Received 6 September 1985; manuscript received in final form 28 January 1986

InP was grown on (001) and (111)B InP substrates by the supercooling and step-cooling technique and $In_{1-x}Ga_xAs_yP_{1-y}$ ($x \sim 0.2$ and $y \sim 0.5$) was grown on (001), (111)A and (111)B InP substrates at 640–650°C by the step-cooling technique. Calculated growth rates assuming diffusion limited growth, using experimental phase diagram relations were compared with experimental data. Excellent agreement was found for the growth of InP on (001) and (111)B InP and for the growth of InGaAsP on (001) InP substrates. For the nucleation of InGaAsP on {111} faces a critical supersaturation of 4°C was observed. The criterion of constant composition for quaternary layers grown at constant temperature was verified using double crystal X-ray diffractometry. A constant composition was observed on the (001) and (111)A faces, in contrast to the (111)B face, where the growth seems to be dictated by surface kinetics.

1. Introduction

Liquid phase epitaxy (LPE) is frequently used to grow thin layers of III–V compounds for optoelectronic devices. From the literature it is clear that the growth rate of binary III–V compounds is determined by the rate of diffusion of group V solutes towards the solid–liquid (S–L) interface. The diffusion limited growth model has been extended to the multicomponent system by de Crémoux [1]. Relations for the layer thickness and the composition of the solid phase were deduced with the aid of linearized phase diagram data. For the growth of InGaAsP lattice matched to InP, diffusion limited growth on (001) InP [2–4] and also orientation effects have been reported [5,6]. Up to now however, no study has been reported in which a quantitative comparison is made between experimental results and the theoretical diffusion limited growth model using experimental phase diagram data of a multicomponent system.

In this report the results of the multicomponent diffusion limited growth model are given in section 2 and experimental methods are described in section 3. In section 4, the experimental results are presented and compared with the diffusion limited growth model for the growth of InP on (001) and (111)B InP substrates by the supercooling and the step-cooling technique and for the growth of InGaAsP on (001), (111)A and (111)B InP substrates by the step-cooling technique.

2. Diffusion limited growth model

The LPE growth rate of III–V compounds has been experimentally determined by many authors and the results have been analysed on the assumption that the growth rate is determined by the rate of solute diffusion towards the S–L interface with fast interface kinetics. If there is no free convection and the area of the growth solution is smaller than or equal to that of the substrate, the mass transfer of solutes towards the S–L interface can be described in the case of an n-component system by $(n-1)$ one-dimensional diffusion equations:

$$D_i \frac{\partial^2 C_i^{\mathrm{L}}(u, t)}{\partial u^2} = \frac{\partial C_i^{\mathrm{L}}(u, t)}{\partial t},$$

$$i = 1, 2, \ldots, n-1, \tag{1}$$

* Eindhoven University of Technology, 5600 MB Eindhoven, The Netherlands.

0022-0248/86/$03.50 © Elsevier Science Publishers B.V.
(North-Holland Physics Publishing Division)

where $C_i^L(u, t)$ is the concentration (atoms/cm^3) of component i in the solution at position u and time t and D_i the diffusion coefficient of component i in the solution (cm^2/s).

The motion of the growing interface is neglected, the diffusion coefficients are assumed to be mutual and concentration independent and the liquidus curve of a multicomponent system is linearized for the small cooling intervals applied.

With these assumptions, as long as the solution may be regarded as semi-infinite ($t \ll d^2/D_i$, where d = the thickness of the solution (cm)), these equations have been previously solved for boundary conditions corresponding to different LPE techniques.

For growth by the supercooling technique the layer thickness e is the sum of the layer thicknesses for the step-cooling and for the equilibrium growth technique:

$$e = K\left(\Delta T\, t^{1/2} + \tfrac{2}{3} R t^{3/2}\right), \tag{2}$$

where ΔT is the initial supersaturation of the solution (°C), R the cooling rate (°C/min), and K the growth rate constant given by

$$K = \frac{2C^L}{\sqrt{\pi}}\left[\sum_{i=1}^{n-1} a_i \frac{C_i^S(0, t) - C_i^L(0, t)}{\sqrt{D_i}}\right]^{-1}, \tag{3}$$

where

$$C^L = \sum_{i=1}^{n} C_i^L,$$

$a_i = \partial T/\partial x_i^L$ is the partial derivative of the liquidus function (°C), and $C_i^S(0, t)$ the concentration (atoms/cm^3) of component i in the solid at the S–L interface at time t (atoms/cm^3).

For the composition of an epitaxial layer grown from a multicomponent solution de Crémoux [1] derived relations using generalized segregation coefficients. He concluded that the growth by the step-cooling technique should result in epitaxial layers with a constant composition. This was experimentally verified by Feng et al. [7].

Therefore, in order to determine whether growth of a multicomponent epitaxial layer occurs in accordance with the diffusion limited growth model there are two things to check for the step-cooling growth technique: the relation expressing the layer thickness as a function of the growth time and supersaturation (eq. (2)), and the constant composition across the thickness.

3. Experimental procedures

3.1. Growth method

The experimental LPE apparatus consisted of a horizontal furnace system and a conventional sliding graphite boat, made from POCO DFP 3-2 graphite. Palladium diffused H_2 flowed through the fused silica reactor tube inside the furnace. Prior to each experiment, the reactor tube was evacuated ($< 5 \times 10^{-2}$ Torr) to remove oxygen and water vapour. The dimensions of the bins were 20×12 mm^2, while the substrates were 22×12 mm^2. To prevent free convection, 3.2 mm thick solutions with graphite blocks on top were used.

For the growth and seed-dissolution experiments, (001), (111)A and (111)B oriented dislocation free InP substrates (S doped, $n = 2 \times 10^{18}$ cm^{-3}) supplied by internal sources [8] were used. The (001) and (111)B substrates were cleaned and etched in a 2% bromine–methanol solution. During the heating the substrates were protected from phosphorus loss by a 4 wt% InP solution in 6N Sn (Billiton) [9]. In the InGaAsP growth experiments an InP buffer layer was grown first to bury any residual damage; in the case of (111)A substrates an In melt-etch was used.

In the seed-dissolution experiments, the solutions were composed of 6N In (Billiton), undoped InAs (MCP) and GaAs (Philips). In the growth experiments undoped InP (MCP) source material was used. Prior to each experiment the In was etched in concentrated HCl and the source materials were batch-wise etched in bromine–methanol. The solutions were homogenized for at least 30 min at 680°C and the seed-dissolution and growth experiments were carried out at 640–660°C. During the seed-dissolution experiments the solution was kept in contact with the substrate for 1 h at constant temperature ($\Delta T < 0.1$°C). In the growth experiments InP layers were grown using the supercooling and the step-cooling technique and

InGaAsP epitaxial layers were grown by the step-cooling technique. All epitaxial layers were not intentionally doped.

3.2. *Characterization of the epitaxial layers*

The thickness of the epitaxial layers was determined at 20 spots using Nomarski phase contrast microscopy for each wafer. Thin epitaxial layers ($e < 0.5$ μm) were measured by means of scanning electron microscopy (SEM).

X-ray diffraction analysis using monochromatic Cu $K\alpha_1$ radiation was performed to determine the relative relaxed mismatch $\Delta a/a$ [10], where $\Delta a = a_q - a$, a_q and a being the lattice constants of the quaternary compound and InP, respectively. For (001) substrates the (004) reflection and for {111} substrates the (222) reflection was used [11].

Photoluminescence measurements were carried out on the surface of the as-grown epitaxial layers at room temperature with standard photoluminescence equipment under low excitation density (200 W/cm^2) using a Kr laser ($\lambda = 647$ nm).

The compositions of the $In_{1-x}Ga_xAs_yP_{1-y}$ epitaxial layers were measured with the electron microprobe analyser (EPMA) "Camebax", with InP and GaAs as standards. The quaternary layer thickness of the analysed samples was always greater than 2 μm to avoid interference from the substrate.

4. Growth experiments

4.1. *Growth of InP on (001) and (111)B InP*

The P concentration in indium in equilibrium with (001) InP, derived from the weight loss of the substrate in seed-dissolution experiments, can be expressed by

$$x_P^L = 2.24 \times 10^3 \exp(-11750/T). \qquad (4)$$

Fig. 1 shows that the difference between our results and earlier published data [12] can be fully attributed to a difference of 9°C in the temperature which was measured under the substrate with a not specially calibrated thermocouple. By a mass balance it was confirmed that no significant

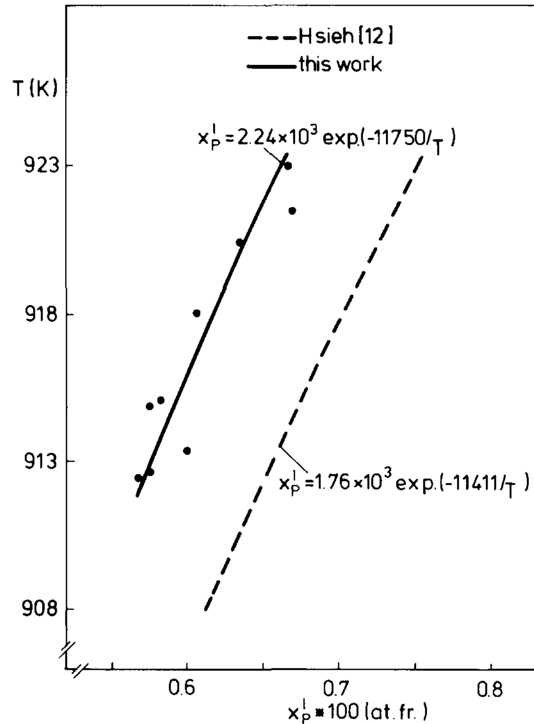

Fig. 1. Part of the liquidus curve of In–P.

evaporation of phosphorus took place during the seed-dissolution experiments.

Growth parameters and layer thicknesses of InP epitaxial layers grown around 650°C on (001) substrates by the supercooling and by the step-cooling technique are shown in table 1. For the growth rate constant of InP on the (001) plane, using eq. (2) we found:

$$K = 0.100 \pm 0.005\ \mu m/°C \cdot min^{1/2}.$$

In experiments where (001) and (111)B InP substrates were put side by side under the same solution we observed that the two InP layer thicknesses did not deviate significantly.

4.2. *Calculation of growth rate of InP*

The growth rate constant is given by eq. (3). In this equation C^L and C^S were calculated from $\rho_{In} = 6.67$ g/cm^3 at 650°C [13] and $\rho_{InP} = 4.787$ g/cm^3 [13], respectively. The diffusion coefficient

Table 1
Results of InP growth on (001) InP substrates

T_g (°C)	ΔT (°C)	R (°C/min)	t (min)	e (μm)	K (μm/°C · min$^{1/2}$)
639.4	3.8	0.40	5	1.1	0.097
640.1	3.5	0.58	6.5	1.5	0.101
647.8	2.7	0.58	12	2.5	0.098
646.5	0.4	0.21	27	2.0	0.092
639.9	2.7	0.56	5	1.1	0.108
650.5	10.8	0	10	3.4	0.100
652.5	8.7	0	10	2.8	0.102

of P in indium is given by [14]:

$$D_P = 17.12 \exp(-11450/T) \text{ cm}^2/\text{s}. \quad (5)$$

Substitution of these data in eq. (3), with our temperature in D_P gives:

$$K = 0.10 \mu\text{m}/°C \cdot \text{min}^{1/2}.$$

From this very good agreement between the calculated and the experimental value it may be concluded that the LPE growth of InP on (001) and (111)B can be described with the one-dimensional diffusion limited growth model.

4.3. Growth of InGaAsP on (001), (111)A and (111)B InP

Seed-dissolution experiments were performed on (001), (111)A and (111)B InP substrates to determine a part of the quaternary (λ_{PL} = 1.2 μm) liquidus curve in the temperature interval of 640–660°C. In these experiments either x^L_{Ga} or x^L_{As} was varied and x^L_P was determined from mass balance (table 2).

Subsequently, InGaAsP epitaxial layers were grown on (001), (111)A and (111)B InP substrates by the step-cooling technique. The composition of the growth solution, as an atomic fraction, in all experiments was: $x^L_{Ga} = 5.54 \times 10^{-3}$, $x^L_{As} = 4.39 \times 10^{-2}$ and $x^L_P = 3.22 \times 10^{-3}$. According to the seed-dissolution experiments, this solution is precisely saturated at 655°C for the (001) face. For the {111} faces the effective saturation temperature was higher by about 2.5°C. This orientation effect on the liquidus temperature was earlier reported for InGaAsP by Oe and Sugiyama [6] and by Nakajima and Akita [15] for InGaAs solutions.

The InGaAsP epitaxial layer thickness grown in 10 min as a function of the supersaturation ($\Delta T = T_L - T_G$) of the growth solution is shown in fig. 2. Only for the (001) face the InGaAsP layer thickness increases linearly, nearly from the origin, with the supersaturation according to eq. (2) with K = 0.13 μm/°C · min$^{1/2}$. The same value of the growth rate constant K was found in experiments where the growth time was varied while the supersaturation was kept constant at 7.7°C. For the growth

Table 2
In–Ga–As–P liquidus compositions determined by seed-dissolution experiments

Orient.	T (°C)	x^L_{Ga}	x^L_{As}	x^L_P
(001)	639.5	0.00452	0.0430	0.00243
(001)	644.8	0.00455	0.0430	0.00277
(001)	655.0	0.00454	0.0430	0.00357
(001)	653.7	0.00454	0.0480	0.00287
(001)	639.5	0.00555	0.0440	0.00227
(001)	644.8	0.00554	0.0439	0.00264
(001)	655.0	0.00554	0.0439	0.00322
(001)	655.0	0.00554	0.0440	0.00321
(001)	653.7	0.00553	0.0479	0.00264
(001)	650.1	0.00550	0.0464	0.00255
(111)B	655.0	0.00553	0.0439	0.00299
(111)B	655.0	0.00455	0.0430	0.00322
(111)B	655.0	0.00559	0.0396	0.00324
(111)B	655.0	0.00459	0.0387	0.00356
(111)B	642.9	0.00557	0.0397	0.00241
(111)B	642.9	0.00459	0.0386	0.00247
(111)B	644.1	0.00555	0.0440	0.00203
(111)B	644.1	0.00453	0.0431	0.00231
(111)A	654.9	0.00551	0.0439	0.00307
(111)A	654.9	0.00437	0.0428	0.00336

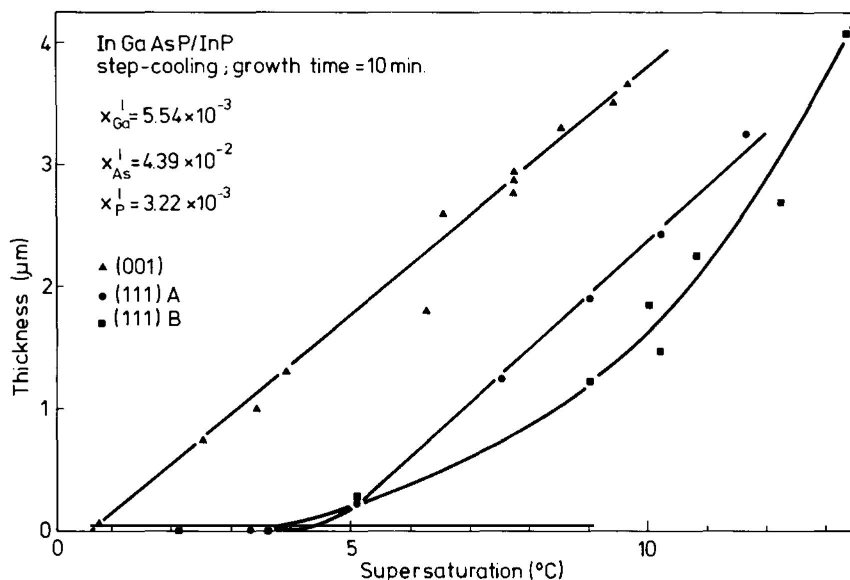

Fig. 2. Layer thickness as a function of the supersaturation for growth by the step-cooling technique, growth time 10 min. The solutions used in all cases are saturated at 655°C for (001), and at 657.5°C for {111} InP substrates.

on {111} faces a critical supersaturation for nucleation of about 4°C was found. Nearly the same critical supersaturation is reported for the growth of InGaAs on {111} InP substrates [16]. For smaller supersaturations and a growth time of 10 min the quaternary layer thickness became less than 0.01 μm, as estimated from EPMA. The InGaAsP layer thickness for the (111)A face, in contrast to the (111)B face, depends linearly on the supersaturation when higher than 5°C. For the (111)A face this results in an effective growth rate constant $K = 0.145\ \mu\text{m}/°\text{C} \cdot \text{min}^{1/2}$.

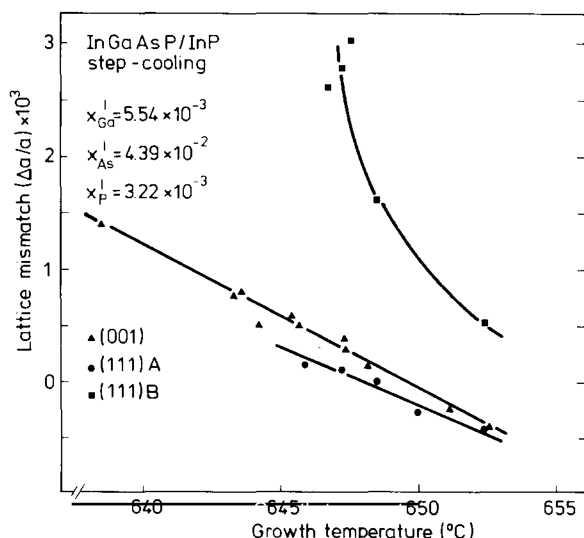

Fig. 3. Dependence of the relative relaxed lattice mismatch on the growth temperature for the step-cooling technique.

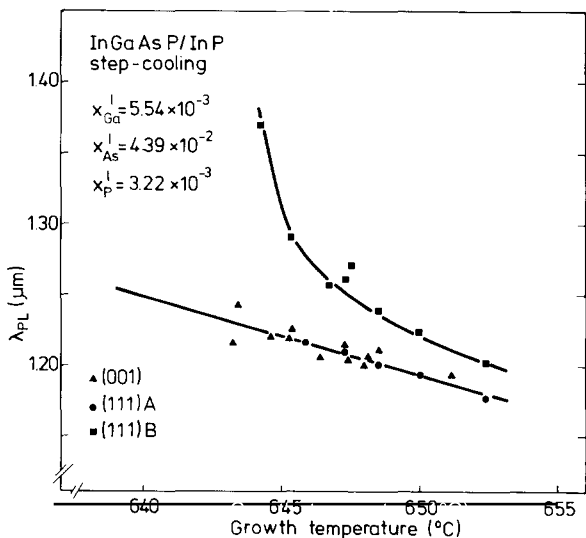

Fig. 4. Dependence of λ_{PL} on the growth temperature for the step-cooling technique.

Figs. 3 and 4 show the relative relaxed mismatch ($\Delta a/a$) and the photoluminescence wavelength (λ_{PL}) of the as-grown InGaAsP epitaxial layers as a function of the growth temperature for the different substrate orientations. The $\Delta a/a$ and λ_{PL} of the quaternary epitaxial layers on (001) and (111)A InP are almost identical and vary linearly with the growth temperature: $(\Delta a/a)/\Delta T = -1.4 \times 10^{-4}/°C$ and $\Delta\lambda_{PL}/\Delta T = -5.3 \times 10^{-3}\ \mu m/°C$ for the (001) face. In fig. 5 the composition of the InGaAsP epitaxial layers grown on (001) InP, as determined by EPMA, is shown as a function of the growth temperature. The composition changes linearly with the growth temperature, predominantly on the group V sublattice. Thus the temperature dependence of the distribution coefficient for the (001) face is larger for the group V atoms, supporting recent results of Matsui et al. [17]. The composition of the individual quaternary epitaxial layers on (001) and (111)A InP substrates is homogeneous across the thickness. This was concluded from double crystal X-ray rocking curves and photoluminescence measurements as shown for a step-cooled grown InGaAsP epitaxial layer on (001) InP in fig. 6. The epitaxial layer was etched off in four steps, (a) to (d), and after each step a double crystal X-ray rocking curve was made and λ_{PL} was measured. All measurements gave the same peak positions, indicating a constant composition across the layer thickness as predicted by the diffusion limited growth model for the step-cooling technique. For comparison, fig. 7 shows the results of a similar etching experiment with an InGaAsP epitaxial layer on (001) InP, of which the first 2 μm was grown in 10 min with the step-cooling technique and then about 1.8 μm in 10 min with linear cooling (R = 0.26°C/min). By etching from (a) to (d), InGaAsP with the larger lattice constant and the larger λ_{PL} is etched off first, which is consistent with figs. 3 and 4.

In figs. 3 and 4 it is clearly shown that the composition of InGaAsP epitaxial layers grown under identical conditions, i.e. with the same com-

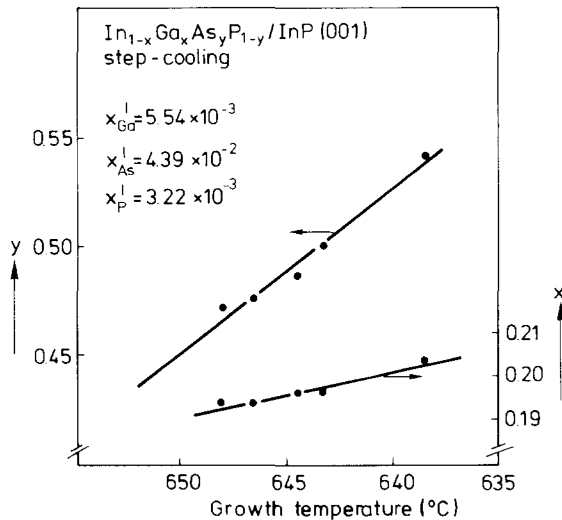

Fig. 5. Dependence of the composition of $In_{1-x}Ga_xAs_yP_{1-y}$ on the growth temperature for the step-cooling technique (accuracy 0.5%).

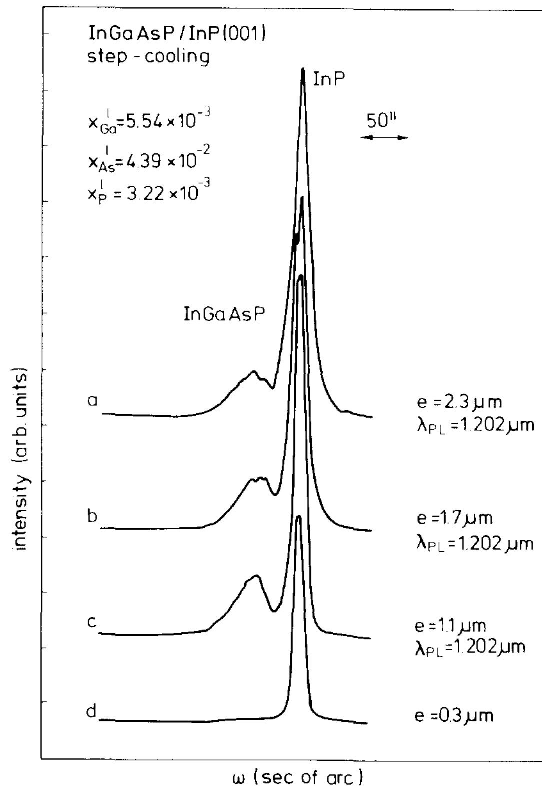

Fig. 6. Double crystal X-ray rocking curves, (004) reflection, of an InGaAsP epitaxial layer grown by the step-cooling technique. Curve (a) is for the as-grown 2.3 μm thick layer. Curves (b), (c) and (d) after etching down to 1.7, 1.1 and 0.3 μm respectively. λ_{PL} was measured after each step.

position of the growth solution and the same growth temperature, differs for the (111)B face from the composition on the (001) and (111)A faces. This difference is strongly temperature dependent. For the (111)B face the distribution coefficient of As is larger than for the (001) and (111)A faces. The double crystal X-ray rocking curves of InGaAsP layers on the (111)B face were very broad, up to 500 sec of arc FWHM for the (222) reflection, and had a lower intensity. From etching experiments performed in the same manner as for the (001) plane it turned out that with increasing growth time, and hence with decreasing supersaturation, the lattice constant and λ_{PL} decreased. This variation of the composition of the solid, and the layer thickness as a function of supersaturation on the (111)B face for the step-cooling technique are clearly not in agreement with the diffusion limited growth model and indicate a significant influence of growth kinetics.

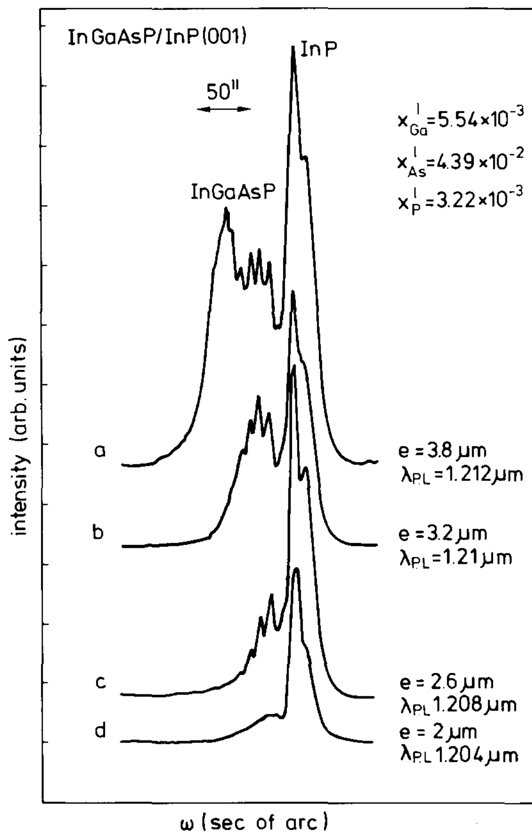

Fig. 7. Double crystal X-ray rocking curves, (004) reflection, of an InGaAsP epitaxial layer composed from first a 2 μm constant composition layer, grown by step-cooling for 10 min. Subsequently 1.8 μm was grown by linear cooling (R = 0.26°C/min) for 10 min. The variation in composition as a function of the thickness is revealed by etching.

The influence of the substrate orientation on the InGaAsP composition was also observed in growth experiments on misoriented substrates. In these experiments two misoriented (001) substrates with the misorientation vector in either the [111]A or the [111]B direction were put side by side under the same solution. Special care was taken during the bromine–methanol etching to keep the proper misorientation. As shown in table 3, the InGaAsP epitaxial layers grown by the step-cooling technique for 10 min on up to 10° in [111] B direction misoriented (001) InP substrates, have a consistently slightly larger lattice constant. This is in agreement with the results obtained on the (111)B face. The linewidth of the double crystal X-ray rocking curves decreases with increasing misorientation, possibly because the terracing disappears and a nearly flat surface is obtained. This holds even more for substrates misoriented in the [111]B direction. A similar behaviour was also observed on nearly exact (001) oriented substrates. The linewidth on a facet had nearly the theoretical value, while the rocking curve of a terraced surface was somewhat broadened. As shown in table 3, the misorientation had no significant influence on the layer thickness.

4.4. *Calculation of the growth rate of InGaAsP (λ_{PL} = 1.2 μm)*

The growth rate constant K (eq. (3)) was calculated with the following experimental data and assumptions:

(a) The partial derivatives of the liquidus function were calculated from the seed-dissolution experiments in the temperature range 640–660°C (table 2). This results in table 4.

(b) The corresponding composition of the epitaxial layers as shown in fig. 5.

(c) In eq. (3), C_i^L (0, t) was neglected.

(d) It was assumed that $D_{As} = D_{Ga} = D_P$. Actual differences between D_{As}, D_{Ga} and D_P by a factor

Table 3
Influence of the substrate misorientation from the (001) face on some parameters of InGaAsP epitaxial layers

Misorientation [a]	$\Delta a/a$	$\Delta\omega$ [b] (seconds or arc)	λ_{PL} (μm)	$\Delta E_{1/2}$ [c] (eV)	e (μm)	ΔT (°C)
< 0.1°	1.4×10^{-4}	40	1.208	1.8 kT	2.9	7.7
1° B	$(1-0.6)\times 10^{-5}$	39	1.208	2 kT	2.9	7.8
1° A	8.5×10^{-5}	–	1.206	2 kT	2.9	7.8
3° B	7.7×10^{-5}	36	1.206	1.8 kT	2.9	7.7
3° A	4.0×10^{-5}	41	1.204	1.8 kT	2.9	7.7
5° B	8.1×10^{-5}	21	1.205	1.8 kT	2.7	7.7
5° A	4.4×10^{-5}	27	1.205	1.8 kT	2.8	7.7
10° B	6.6×10^{-5}	19	1.206	1.7 kT	2.7	7.7
10° A	2.0×10^{-5}	28	1.206	1.7 kT	2.9	7.7
10° B	-3.69×10^{-4}	20	1.18	2 kT	1.0	3.4
10° A	-3.84×10^{-4}	21	1.19	2 kT	1.0	3.4

[a] Notation: A, B: misorientation from (001) in [111]A, [111]B direction, respectively
[b] FWHM of double crystal X-ray rocking curve, (004) reflection. For the nominal (001) substrates average of about 30 experiments.
[c] FWHM of photoluminescence peak at room temperature.

of 2 account for only a few percent difference in the calculated K value.

Using these data, the InGaAsP ($\lambda_{PL} = 1.2$ μm) growth rate constant $K = 0.127 \pm 0.004$ μm/°C · min$^{1/2}$ was obtained for the (001) face and $K = 0.185 \pm 0.005$ μm/°C · min$^{1/2}$ for the (111)A face. The results on the (001) face are in excellent agreement with the experimentally determined value.

5. Discussion

The Kossel model for crystal growth distinguishes between diffusion of the solute species towards the growing interface, adsorption, surface-diffusion and incorporation into the crystal lattice. If the first diffusion step is the rate-limiting, the growth can be described with the diffusion limited growth model. The results of this study show that this holds for LPE growth of InP on (001) and (111)B substrates and for the growth of InGaAsP ($\lambda_{PL} = 1.2$ μm) on the (001) InP face. For the LPE growth of InGaAsP ($\lambda_{PL} = 1.2$ μm) on the {111} InP faces a critical supersaturation for nucleation is observed. Similar results for InGaAs growth on {111} InP faces have been reported by Yamazaki et al. [16].

The difference between the ease of nucleation for the {001} and {111} planes in the zincblende lattice can be explained by an attachment model as discussed by Sangster [18]. He considered the adsorption of a single atom on different planes and calculated the variation in the number of the dangling bonds. If the number of dangling bonds increases the adsorption of an atom would be rather improbable. For the (001) plane, group III as well as group V atoms can attach without creating extra dangling bonds; so no nucleation problems are expected.

The {111} planes consist of double layers of tightly bound group III and group V atoms. Each atom in a plane makes bonds to three nearest neighbour atoms in the other plane. The fourth

Table 4
Partial derivatives of the liquidus function

Orientation	$\partial T/\partial x_P^L$ (°C)	$\partial T/\partial x_{As}^L$ (°C)	$\partial T/\partial x_{Ga}^L$ (°C)
(001)	1.63×10^4	2050	3200
{111}	1.15×10^4	800	2500

bond extends normal to the planes to combine with the adjacent double layers. Adsorption of opposite type atoms, compared to the surface atoms, will be improbable because each atom creates a net addition of two dangling bonds, which is energetically unfavourable; this situation should also result in a deviation from stoichiometry. An energetically more favourable situation is the creation of a smallest portion of the double layer, which consists of at least three atoms of the opposite type and one atom of the same type as the original surface. For further nucleation the adsorption of a single atom on the original surface next to this centre is required, where again two dangling bonds are created. Subsequently, a series of group III and group V atoms can readily be added to the crystal with two bonds. This process has to be repeated at the start of the growth of every new chain. With these models the observed difference in nucleation of InGaAsP, InGaAs [16] and InGaP [19] on {001} and {111} planes can be qualitatively explained.

The growth of InGaAsP on the (111)A face might be described with the diffusion limited growth model once the nucleation barrier has been overcome. For the step-cooling technique the layer thickness depends linearly on the supersaturation (fig. 2) and the composition of the solid is homogeneous, but a rather large difference between the experimentally determined growth rate constant and the calculated one is found. For the (111)B face the growth seems to be dictated by surface kinetics over the full temperature range. A rather poor homogeneity of the solid grown on the (111)B face is also reported for InGaP/GaAs [20] and InGaAsP/GaAs [21].

The large critical supersaturation for nucleation of InGaAsP and InGaAs on {111} faces is not observed for InP (this work), GaAs and AlGaAs [22] indicating that attachment of atoms on {111} planes is not as difficult in all systems. The observed differences may be attributable to III–V complexes which might be present in the solution. The liquid interaction parameters [23] and the differences in activation energies for diffusion and dissolution of group V atoms in group III solutions [24] indicate that the interaction between III–V atoms decreases in going from InAs, GaAs, GaP to InP. In the last case there is effectively no interaction.

6. Conclusions

We have shown that the growth of InP on (001) and (111)B InP by the supercooling and step-cooling technique and the growth of InGaAsP (λ_{PL} = 1.2 μm) on (001) InP substrates, up to 10° misorientation in $\langle 111 \rangle$, by the step-cooling technique can be described with the diffusion limited growth model and the extended multicomponent model using linearized phase diagram data. For the growth of InGaAsP on {111} InP substrates a critical supersaturation for nucleation of 4°C is observed. This may qualitatively be explained with an attachment model of atoms, but it also seems necessary to take into account III–V complexes in the growth solution. Above the critical supersaturation the growth of InGaAsP on the (111)A face seems to be diffusion limited, in contrast to the (111)B face, where the growth appears to be dictated by surface kinetics. For the (111)B face the distribution coefficient of As is larger than for the (001) and (111)A faces. For the (001) face the group V element distribution coefficients show a stronger temperature dependence than the group III elements.

Acknolwedgments

The authors are indebted to W.J. Bartels and D.J.W. Lobeek for double crystal X-ray diffraction measurements, to Mrs. W. Dijksterhuis and P.I. Kuindersma for photoluminescence measurements, and to J.A. de Poorter for SEM analyses.

References

[1] B. de Crémoux, in: Proc. 7th Intern. Symp. on GaAs and Related Compounds, St. Louis, 1978, Inst. Phys. Conf. Ser. 45, Ed. C.M. Wolfe (Inst. Phys., London–Bristol, 1979) pp. 52–60.

[2] M. Feng, L.W. Cook, M.M. Tashima and G.E. Stillman, J. Electron. Mater. 9 (1980) 241.

[3] L.W. Cook, M.M. Tashima and G.E. Stillman, J. Electron. Mater. 10 (1981) 119.

[4] E.A. Rezek, B.A. Vojak, R. Chin and N. Holonyak, Jr., J. Electron. Mater. 10 (1981) 255.
[5] J.J. Hsieh, M.C. Finn and J.A. Rossi, in: Proc. North American Session of 6th Intern. Symp. on GaAs and Related Compounds, St. Louis, 1976, Inst. Phys. Conf. Ser. 33b, Ed. L.F. Eastman (Inst. Phys., London–Bristol, 1977) pp. 37–44.
[6] K. Oe and K. Sugiyama, Appl. Phys. Letters 33 (1978) 449.
[7] M. Feng, L.W. Cook, M.M. Tashima, T.H. Windhorn and G.E. Stillman, Appl. Phys. Letters 34 (1979) 292.
[8] P.J. Roksnoer and M.M.B. van Rijbroek-van den Boom, J. Crystal Growth 66 (1984) 317.
[9] G.A. Antypass, Appl. Phys. Letters 37 (1980) 64.
[10] J. Hornstra and W.J. Bartels, J. Crystal Growth 44 (1978) 513.
[11] W.J. Bartels, J. Vacuum Sci. Technol. B1 (1983) 338.
[12] J.J. Hsieh, in: Proc. North American Session of 6th Intern. Symp. on GaAs and Related Compounds, St. Louis, 1976, Inst. Phys. Conf. Ser. 33b, Ed. L.F. Eastman (Inst. Phys., London–Bristol, 1977) pp. 74–80.
[13] Handbook of Chemistry and Physics, 63rd ed. (CRC Press, 1982).
[14] K. Nakajima, S. Yamazaki and K. Akita, J. Crystal Growth 56 (1982) 547.
[15] K. Nakajima and K. Akita, J. Electrochem. Soc. 129 (1982) 2603.
[16] S. Yamazaki, K. Nakajima and Y. Kishi, Fujitsu Sci. Tech. J. 20 (1984) 329.
[17] J. Matsui, K. Onabe, T. Kamejima and I. Hayashi, J. Electrochem. Soc. 146 (1979) 664.
[18] R.C. Sangster, in: Compound Semiconductors, Vol. 1, Preparation of III–V Compounds, Eds. R.K. Willardson and H.L. Goering (Reinhold, New York, 1962).
[19] M. Kume, J. Ohta, N. Ogasawara and R. Ito, Japan. J. Appl. Phys. 21 (1982) L424.
[20] H. Asai and K. Oe, J. Crystal Growth 62 (1983) 67.
[21] S. Kaneiwa, T. Takenaka, S. Yana and T. Hijikata, J. Crystal Growth 62 (1983) 498.
[22] P.J.A. Thijs, unpublished results, 1984.
[23] E.H. Perea and C.G. Fonstad, J. Electrochem. Soc. 127 (1980) 313.
[24] S. Iyer, E.K. Stefanakos, A. Abul-Fadl and W.J. Collis, J. Crystal Growth 67 (1984) 337.